



# Feasibility of computed tomography texture analysis of hepatic fibrosis using dual-energy spectral detector computed tomography

ByukGyung Choi<sup>1</sup> · In Young Choi<sup>1</sup> · Sang Hoon Cha<sup>1</sup> · Suk Keu Yeom<sup>1</sup> · Hwan Hoon Chung<sup>1</sup> · Seung Hwa Lee<sup>1</sup> · Jaehyung Cha<sup>2</sup> · Ju-Han Lee<sup>3</sup>

Received: 15 May 2020 / Accepted: 6 July 2020 / Published online: 14 July 2020  
© Japan Radiological Society 2020

## Abstract

**Purpose** To evaluate feasibility of computer tomography texture analysis (CTTA) at different energy level using dual-energy spectral detector CT for liver fibrosis.

**Materials and methods** Eighty-seven patients who underwent a spectral CT examination and had a reference standard of liver fibrosis (histopathologic findings,  $n = 61$ , or clinical findings for normal,  $n = 26$ ) were included. Mean gray-level intensity, mean number of positive pixels (MPP), entropy, skewness, and kurtosis using commercially available software (TexRAD) were compared at different energy levels. Optimal CTTA parameter cutoffs to diagnose liver fibrosis were evaluated. CTTA parameters at different energy levels correlated with liver fibrosis. The association of CTTA parameters with energy level was evaluated.

**Results** Mean gray-level intensity, skewness, kurtosis, and entropy showed significant differences between patients with and without clinically significant hepatic fibrosis ( $P < 0.05$ ). Mean gray-level intensity at 50 keV was significantly positively correlated with liver fibrosis ( $\rho = 0.502$ ,  $P < 0.001$ ). To diagnose stages F2–F4, entropy and mean gray-level intensity at low keV level showed the largest area under the curve (AUC; 0.79 and 0.79). Estimated marginal means (EMMs) of mean gray-level intensity showed prominent differences at low energy levels.

**Conclusion** CTTA parameters from different keV levels demonstrated meaningful accuracy for diagnosis of liver fibrosis or clinically significant hepatic fibrosis.

**Keywords** Texture analysis · Dual-energy spectral CT · Liver · Fibrosis · Quantitative imaging

---

✉ In Young Choi  
ciy1114@naver.com

ByukGyung Choi  
chlqrrudk@gmail.com

Sang Hoon Cha  
sahcha@korea.ac.kr

Suk Keu Yeom  
pagoda20@hanmail.net

Hwan Hoon Chung  
chungmic@korea.ac.kr

Seung Hwa Lee  
gareureung@daum.net

Jaehyung Cha  
dolcha@korea.ac.kr

Ju-Han Lee  
repath@korea.ac.kr

- <sup>1</sup> Department of Radiology, Korea University College of Medicine, 123 Jeokgeum-ro, Danwon-gu, Ansan 15355, Republic of Korea
- <sup>2</sup> Department of Biostatistics, Korea University College of Medicine, 123 Jeokgeum-ro, Danwon-gu, Ansan 15355, Republic of Korea
- <sup>3</sup> Department of Pathology, Korea University Ansan Hospital, Korea University College of Medicine, 123 Jeokgeum-ro, Danwon-gu, Ansan 15355, Republic of Korea

## Introduction

Chronic liver disease (CLD) has a variety of causes, including viral infection [hepatitis B virus, HBV, and hepatitis C virus (HCV)], alcoholic liver disease, nonalcoholic fatty liver, and autoimmune hepatitis [1, 2]. Among the etiologies, 257 million and 71 million people (3.5% and 1% of the population, respectively) suffered from chronic HBV and HCV infections globally in 2015, respectively. In particular, the African and Western Pacific regions harbor 68% of HBV infections [3]. Diagnosing the precise fibrosis stage is essential for HBV- or HCV-induced CLD because there is potential for reversal or prevention of progression to advanced fibrosis or cirrhosis and the associated complications of hepatocellular carcinoma (HCC) and portal hypertension (e.g., varices), which are important causes of morbidity and mortality in CLD patients [4, 5].

The gold standard for diagnosing exact hepatic fibrosis grade is based on pathology of liver biopsy [6, 7]. However, many limitations of liver biopsy, including procedure-related complications, relatively high cost, sampling error, and interobserver variability, have been obstacles for long-term management of CLD [5, 8]. Many non-invasive techniques have been introduced to assist the management process, including ultrasound elastography (USE) and MR elastography (MRE). Although those modalities have proven useful in actual medical practice, operator, technique, and patient-related dependency may affect the outcomes. In addition, the high cost of MRE is a deterrent as a screening or follow-up tool for CLD [5, 9]. Thus, there has been growing clinical need for objective, or quantitative, non-invasive imaging biomarkers to determine and assess hepatic fibrosis stage.

Computed tomography texture analysis (CTTA) is a tool that analyzes the distribution and relationship of pixel or voxel gray levels in the region of interest (ROI) and produces objective and quantitative data without affecting the patient or further imaging studies. CTTA allows more objective assessment of lesion or organ heterogeneity beyond the limit of the naked eye [10]. CTTA has shown potential in assessing various tumors, including renal cell carcinoma (RCC), liver masses, pancreatic cystic lesions, and colorectal polyps [11–14], as well as response evaluation [10]. In addition, CTTA shows probable effectiveness for evaluating non-oncologic diseases including hepatic fibrosis stage [10, 15].

Dual-energy CT (DECT) provides simultaneous image acquisition at two different energy levels, providing information regarding tissue composition and the way tissue changes at different energy levels [15–17]. Various energy levels in monoenergetic CT images show diverse effects on different CTTA parameters. Therefore, specific energy

levels must be tailored to the specific disease for quantifying and assessing the lesion, thus showing greater comparability [16]. Lubner et al. showed that mean gray-level intensity increased with fibrosis stage [15]. Low energy levels in monoenergetic CT images enhance the photoelectric attenuation of iodine [17]. Differences in CTTA parameters of the liver between patients with hepatic fibrosis and those without it could be greater at different energy levels in monoenergetic CT images, especially low energy levels. The purpose of this study was to evaluate the feasibility of CTTA of the liver at different energy levels using a dual-energy spectral detector CT for assessing liver fibrosis.

## Materials and methods

### Patients

This retrospective study was approved by the institutional review board (IRB) with waiver of informed patient consent. Review of the institutional radiology database from July 2016–August 2018 revealed 94 patients with liver parenchymal biopsy-confirmed chronic liver disease who underwent liver dynamic CT scan with a dual-energy spectral detector CT (iQON Spectral CT, Philips Healthcare, Best, Netherlands). Among the patients, 33 were excluded for the following reasons: (1) etiology other than HBV or HCV ( $n=22$ ); (2) no available contrast-enhanced CT image obtained more than 1 year after or before biopsy ( $n=7$ ); and (3) incidental focal lesion, more than 2 cm ( $n=4$ ). Normal patients were clinically asymptomatic patients who underwent liver dynamic CT scan with a dual-energy spectral detector CT at a health examination center. The inclusion criteria for patients with clinically normal liver were: (1) CT scan with a dual-energy spectral detector CT for evaluation of benign hepatic lesion or benign gallbladder lesion and (2) normal liver function test results and negative viral serology test results obtained within 1 month of the CT examination. The final study population comprised 87 patients (54 males and 33 females; mean age  $\pm$  standard deviation, SD,  $53.59 \pm 10.7$  years; Fig. 1).

### Histopathologic analysis

All liver samples were biopsied within 1 year of liver dynamic CT (median interval = 0 day, interquartile range [IQR], from  $-120$  to 20 days). The samples were staged using the METAVIR scoring system [18], where F0 indicated no fibrosis, F1 indicated portal fibrosis without septa, F2 indicated portal fibrosis with rare septa, F3 indicated numerous septa without cirrhosis, and F4 indicated cirrhosis [19].

**Fig. 1** Flow chart of the study population. *CT* computed tomography, *CLD* chronic liver disease

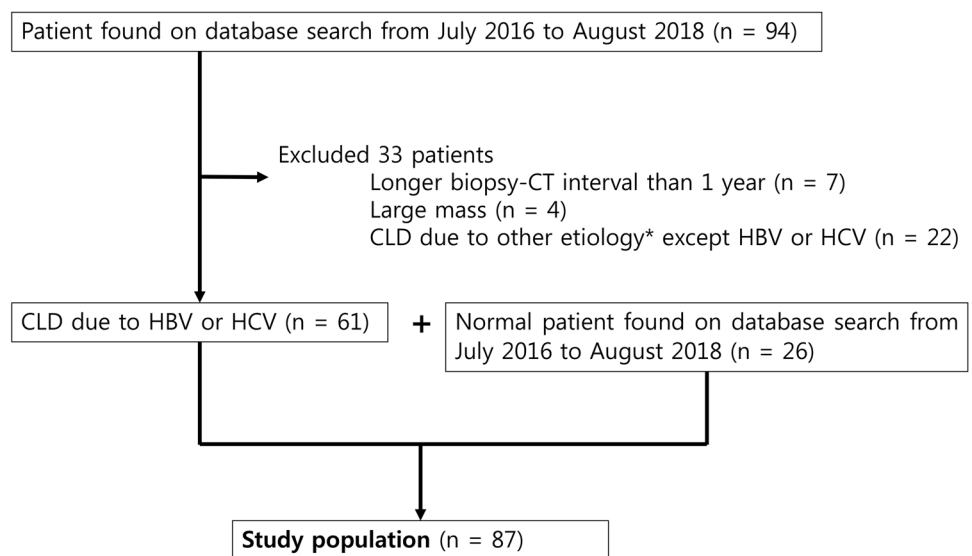


**Table 1** Dual-energy computed tomography acquisition parameters

Parameters	Dual-energy spectral CT
Tube voltage (kVp)	120
Tube current (mA)	Automated tube current modulation
Rotation time (s)	0.4
Helical pitch	0.891
Contrast injection dose	120 ml of 350 mg/ml (2 ml/kg)
Contrast injection rate (ml/s)	3.5 ml/s
Contrast injection duration (s)	34 s

### MDCT technique

CT scans were performed using a dual-energy spectral detector CT with tube potential of 120 kV and a matrix of  $512 \times 512 \times 16$ . All CT scans were performed using automated tube potential, and the slice thickness was 3 mm. For CTTA measurement, portal venous phase (acquired at 70 s after contrast injection) images were used (Table 1) [20, 21], which showed CTTA of the liver in this phase to be effective. While delayed phases may emphasize fibrosis [22], portal venous phase is the basic protocol in abdomen and pelvis CT (APCT) for most institutions and is a candidate for a widely applicable imaging biomarker.

Based on several other whole liver studies, a representative single-slice image was selected at the level where portal vein bifurcated and both hepatic lobes were visualized [20, 21, 23]. The selected axial virtual monoenergetic images (VMIs) were processed with a Philips IntelliSpace Portal program 9.0 at five different energy levels (50 keV, 60 keV, 70 keV, 80 keV, 90 keV) (Fig. 2). A total of 435 axial CT images (87 axial scan images  $\times$  5 different keV levels) were selected for CTTA analysis.

### Computed tomography texture analysis (CTTA)

CTTA was performed by a single radiologist with 12 years of experience in abdominal imaging interpretation who was blinded to the clinical information. The selected reconstructed DICOM single-slice images were transferred to a commercially available texture analysis research software platform (TexRAD Ltd, part of Feedback Plc, Cambridge, UK). Using the software, an ROI was manually drawn on each image at 70 keV to cover the entire liver except major vessels and ribs and was copied to other keV images (50 keV, 60 keV, 80 keV, 90 keV) of the same patient (Fig. 3). In addition, the CTTA algorithm performs an excluding procedure that removes any pixels corresponding to areas of fat, air, and major vessels with CT number beyond the range of 0–300 HU [16]. Whether to analyze single-slice or multi-slice or volume data is not established yet, but single-slice image data acquisition is adopted in many previous studies, and it is less laborious and more practical [15, 23–26]. A Laplacian of Gaussian (LoG) spatial band-pass (monorthogonal wavelet) filter was used in the present study as a filtration histogram technique of this software. The filter helps to extract and enhance features of diverse sizes and intensity variation [27, 28]. The derived images from filtration show features ranging from fine (spatial scaling factor, SSF 2, which refers to object radius of 2 mm), to medium (SSF 3, 4, and 5, which refer to respective object radii of 3, 4, and 5 mm), to coarse (SSF 6, which refers to object radius of approximately 6 mm) texture maps [23, 29]. The Histogram-based statistical parameter quantity values were produced at each SSF, including mean gray-level intensity, SD (dispersion from the mean), entropy (irregularity), mean of positive pixels (MPP), skewness (asymmetry), and

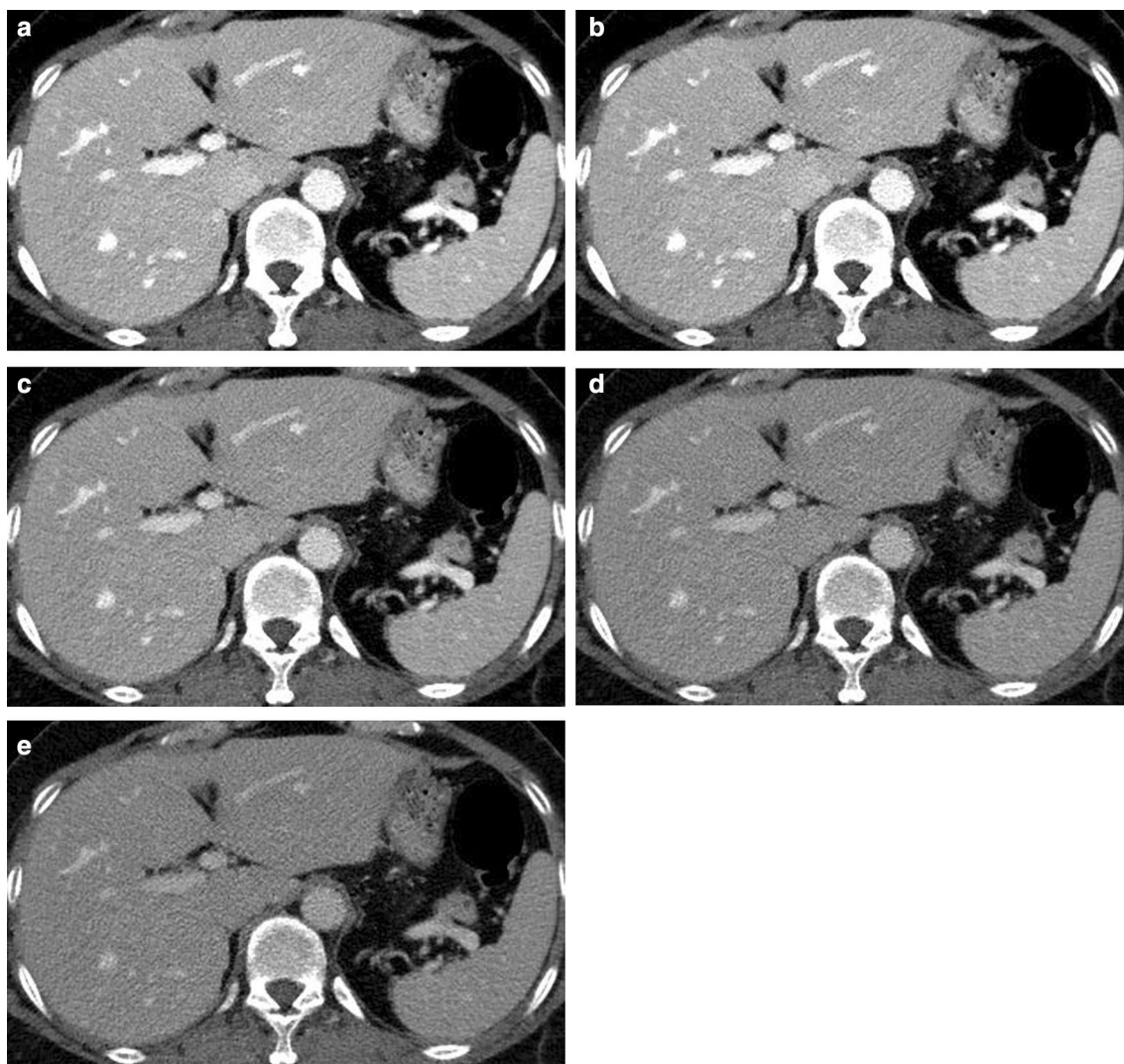


**Fig. 2** Representative computed tomography images at 50 keV (a), 60 keV (b), 70 keV (c), 80 keV (d), 90 keV (e) levels. The selected axial virtual monoenergetic images at portal phase were processed

with a Philips IntelliSpace Portal program 9.0 at five different energy levels (50 keV, 60 keV, 70 keV, 80 keV, 90 keV levels)

kurtosis (peakedness or sharpness). The texture features had some interrelationships with stage of hepatic fibrosis.

### Statistical analysis

Repeated measures ANOVA was used to evaluate differences in CTTA parameters among F0–F4 depending on keV group. The correlations between CTTA parameters based on severity of hepatic fibrosis were evaluated using Spearman's rank correlation test. The differences among CTTA parameters between patients with clinically significant hepatic fibrosis (F2–F4) and patients without clinically significant hepatic fibrosis (F0–F1) were assessed using the Mann–Whitney test.

Optimal CTTA parameter cutoffs for diagnosing clinically significant hepatic fibrosis (F2–F4), advanced fibrosis (F3–F4), and cirrhosis (F4) were evaluated using receiver operating characteristic (ROC) curve analysis for all SSFs (2, 3, 4, 5, 6) and keV (50,60,70,80,90) combinations. The AUC was calculated using DeLong 95% confidence interval (CI). The Mann–Whitney test, Kruskal–Wallis test, one-way ANOVA, and estimated marginal means with repeated measures ANOVA were used to analyze the associations of CTTA parameters with energy level. The independent Student's *t* test was used to analyze differences of CTTA parameters between HBV and HCV patients.

Statistical analyses were performed using SPSS version 25.0 (IBM SPSS, Armonk, NY, USA) and MedCalc version 18.11 (MedCalc Software bvba, Ostend, Belgium).

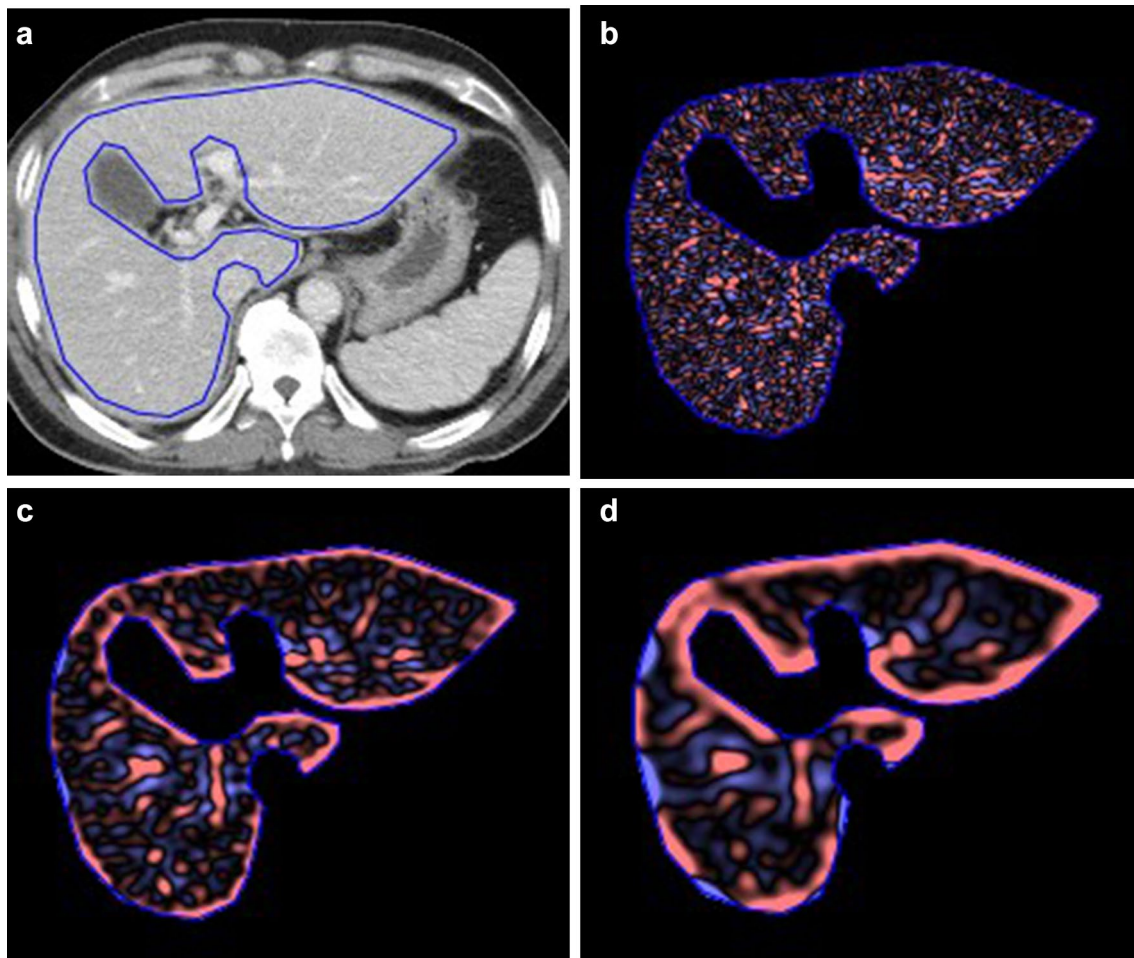


**Fig. 3** Illustration of regions of interest (ROIs) of computed tomography (a) and corresponding texture images at spatial scaling factors (SSFs) of 2 (b), 4 (c), and 6 (d). The portal phase image shows relatively normal liver in a 52-year old male who was histopathologically

confirmed as F2 METAVIR fibrosis score. The color overlay represents general attenuation of the pixels: pink or red=positive pixels, blue or purple=negative pixels (color figure online)

A  $P$  value  $< 0.05$  was considered to indicate significant difference.

## Results

### Patients

The clinical and histologic characteristics of the study population are summarized in Table 2. Among the 87 patients, 61 had chronic liver disease, and 26 were clinically normal.

### CTTA parameter distribution based on severity of hepatic fibrosis

All parameters of mean gray-level intensity, skewness, kurtosis, entropy, SD, and MPP at 50 keV, 60 keV, 70 keV, 80 keV, and 90 keV levels at all SSFs (total of  $87 \times 5$

**Table 2** Patient characteristics

Characteristic	Number of patients ( $n=87$ )
Age, years (mean $\pm$ SD, range)	53.59 $\pm$ 10.7 (29–84)
Sex	
Male	54
Female	33
Etiology (in CLD patients)	61
Hepatitis B virus	34
Hepatitis C virus	27
Clinically asymptomatic patients	26
Histologic grade of hepatic fibrosis (METAVIR score)	
F1	15
F2	20
F3	11
F4	15

SD standard deviation, CLD chronic liver disease

(keV)  $\times$  5 (SSF)  $\times$  6 (parameters) = 13,050 dataset, supplementary data) differed significantly based on severity of hepatic fibrosis (F0–F4;  $P < 0.008$ ). Mean gray-level intensity, skewness, kurtosis, and entropy showed significant differences between patients with and without clinically significant hepatic fibrosis ( $P < 0.05$ ). SD and MPP did not show significant differences ( $P > 0.097$ ) except SD at SSF6 with 60 keV, 70 keV, 80 keV, 90 keV energy levels, and MPP at SSF 6 with 80 keV, 90 keV. Kurtosis and mean grey level intensity at 50 keV in patients with clinically significant hepatic fibrosis were greater than in patients without clinically significant hepatic fibrosis ( $P < 0.001$ ). Mean gray-level intensity at 50 keV, 60 keV, 70 keV, 80 keV, and 90 keV in patients with clinically significant hepatic fibrosis was greater than in patients without clinically significant hepatic fibrosis ( $P < 0.001$ , Fig. 4). Entropy at 50 keV, 60 keV, and 70 keV in patients with clinically significant hepatic fibrosis was smaller than in patients without clinically significant hepatic fibrosis ( $P < 0.001$ ; Table 3).

Mean gray-level intensity at all 25 combination of energy level and SSF, showed a statistically significant positive correlation with hepatic fibrosis stage; the strongest correlation was observed for mean gray-level intensity at 50 keV with medium feature size SSF 4 ( $\rho = 0.502$ ,  $P < 0.001$ ), followed by at 50 keV with medium feature size SSF 5 ( $\rho = 0.496$ ,  $P < 0.001$ ) and at 50 keV with coarse feature size SSF 6 ( $\rho = 0.468$ ,  $P < 0.001$ ).

**Table 3** CTTA parameters based on hepatic fibrosis

Energy level (keV)	SSF	Parameters	CSHF (mean, $n = 41$ )	No CSHF (mean, $n = 46$ )	$P$ value
50	2	Kurtosis	53.97	32.82	<0.001
50	2	Mean	53.62	33.21	<0.001
50	4	Mean	55.72	30.85	<0.001
50	6	Entropy	32.13	57.32	<0.001
50	6	Mean	54.65	32.05	<0.001
60	2	Mean	52.28	34.71	0.001
60	4	Mean	54.13	32.63	<0.001
60	6	Entropy	32.61	56.78	<0.001
60	6	Mean	53.13	33.76	<0.001
70	4	Mean	52.57	34.39	0.001
70	6	Entropy	34.17	55.02	<0.001
70	6	Mean	52.83	34.1	0.001
80	4	Mean	52.28	34.71	0.001
80	6	Mean	52.91	34	<0.001
90	6	Mean	52.54	34.41	0.001

CSHF clinically significant hepatic fibrosis (F2–F4), CTTA computed tomography texture analysis, SSF spatial scaling factor, MEAN mean gray-level intensity

\*\*Only  $P$  values  $\leq 0.001$  are displayed

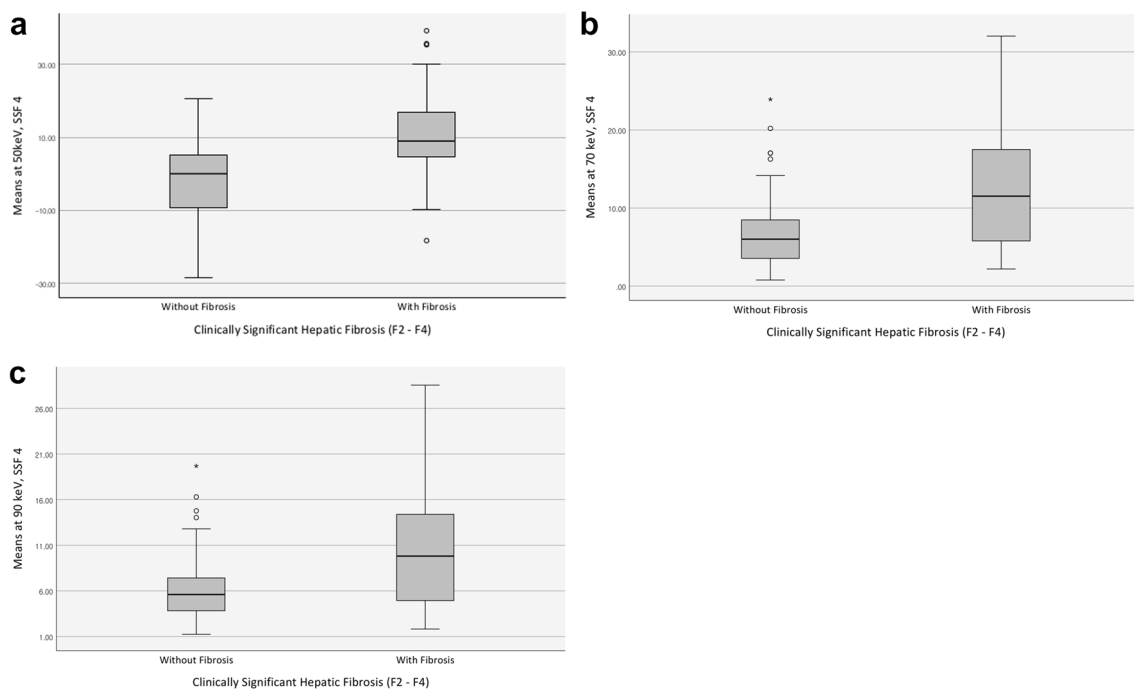


**Fig. 4** Computed tomography texture analysis (CTTA) parameters based on hepatic fibrosis. The box plots show significant differences between patients with and without clinically significant hepatic fibro-

sis for mean gray-level intensity at spatial scaling factor 4 (SSF 4) and energy levels 50 keV (a), 70 keV (b), and 90 keV (c)

Kurtosis at all five energy levels with fine feature size SSF 2, at 50 keV with SSF 3, 6, and at 60 keV with SSF 6, showed a statistically significant positive correlation with hepatic fibrosis stage; the strongest correlation was observed for kurtosis at 50 keV with SSF 2 ( $\rho=0.432, P<0.001$ ), followed by 90 keV with SSF 2 ( $\rho=0.430, P<0.001$ ).

Entropy at coarse feature size SSF 6 with 50 keV, 60 keV, 70 keV, and 80 keV energy levels, and SSF 2 with 90 keV energy level, showed a statistically significant negative correlation with hepatic fibrosis stage; the strongest correlation was observed for entropy at 50 keV with SSF 6 ( $\rho=0.423, P<0.001$ ), followed by 60 keV with SSF 6 ( $\rho=0.382, P<0.001$ ).

Skewness at the 50 keV level with SSF 2, 3, 4, 5, and 60 keV, 70 keV, 80 keV and 90 keV with SSF 4, 5, 6, showed a statistically significant positive correlation with hepatic fibrosis stage; the strongest correlation was observed for skewness at 50 keV level with medium feature size SSF 4 ( $\rho=0.305, P=0.004$ ), followed by at 50 keV with medium feature size SSF 3 ( $\rho=0.300, P=0.005$ ).

### Diagnostic performance of CTTA parameters for diagnosis of hepatic fibrosis

To diagnose the presence of fibrosis (F1–F4), kurtosis at the 90 keV level and mean gray-level intensity at the 50 keV and 70 keV levels showed the largest AUC (0.80, 0.80, and 0.80, respectively), in particular SSF 2, 3, and 4, as shown in Table 4. To diagnose significant fibrosis (F2–F4), entropy and mean gray-level intensity at the 50 keV level

showed the largest AUC (0.79 and 0.79, respectively). To stage advanced fibrosis (F3–F4), skewness at the 80 keV level showed the largest AUC (0.78). To stage cirrhosis (F4), kurtosis showed the largest AUC (0.79), followed by skewness and mean gray-level intensity (AUC; 0.76 and 0.75, respectively; Table 4).

### Relationships of CTTA parameters with energy level

Mean gray-level intensity at medium feature size SSF 4 and entropy at coarse feature size SSF 6 showed relatively fair diagnostic performance ( $P<0.001$  and  $P<0.01$ , respectively) for clinically significant hepatic fibrosis (F2–F4) at all five energy levels. Mean gray-level intensity and entropy showed significant difference ( $P=0.005$  and  $P<0.001$ , respectively) among low, intermediate, and high energy levels (50 keV, 70 keV, 90 keV). Average mean gray-level intensity increased proportionally among low, intermediate, and high energy levels (4.35, 8.58, and 10.27, respectively). In addition, average entropy decreased proportionally among low, intermediate, and high energy levels (5.85, 5.33, and 5.00, respectively) with significant differences ( $P<0.001$ ).

Estimated marginal mean (EMM) of mean gray-level intensity at medium feature size SSF 4 tended to show prominent differences among hepatic fibrosis scores at the low energy level (50 keV) (Fig. 5). The EMM of entropy at coarse feature size SSF 6 tended to decrease in reverse proportion to energy level. The EMM of kurtosis at medium feature size in cirrhosis showed a rapid increase as energy level increased, unlike other fibrosis grades. The EMM of

**Table 4** Results of ROC curve analysis for diagnosing hepatic fibrosis

Parameter	Energy level	SSF	Fibrosis stage	AUC	95% CI	P value	Cutoff value	Sensitivity (%)*	Specificity (%)*
Kurtosis	90	2	F1–F4	<b>0.80**</b>	0.702, 0.879	<0.001	> 5.48	54.1	100
Mean	70	3	F1–F4	<b>0.80**</b>	0.700, 0.877	<0.001	> 3.68	63.93	92.31
Mean	50	4	F1–F4	<b>0.80**</b>	0.699, 0.877	<0.001	> 3.34	73.77	80.77
Mean	70	2	F1–F4	0.79	0.693, 0.872	<0.001	> 1.05	60.66	92.31
Mean	50	5	F1–F4	0.78	0.678, 0.862	<0.001	> 15.39	62.3	88.46
Entropy	50	6	F2–F4	<b>0.79**</b>	0.689, 0.870	<0.001	< 5.53	71.74	75.61
Mean	50	4	F2–F4	<b>0.79**</b>	0.685, 0.867	<0.001	> 3.34	82.61	70.73
Mean	50	5	F2–F4	0.78	0.676, 0.860	<0.001	> 16.48	65.22	80.49
Mean	50	3	F2–F4	0.77	0.665, 0.852	<0.001	> -0.44	67.39	80.49
Mean	50	6	F2–F4	0.76	0.656, 0.845	<0.001	> 17.03	82.61	60.98
Skewness	80	5	F3–F4	<b>0.78**</b>	0.675, 0.859	<0.001	> 2.36	65.38	81.97
Kurtosis	60	2	F4	<b>0.79**</b>	0.689, 0.869	<0.001	> 8.17	80	77.78
Skewness	80	6	F4	0.76	0.652, 0.842	<0.001	> 3.27	66.67	80.56
Mean	50	6	F4	0.75	0.64, 0.835	<0.001	> 29.6	86.67	66.67

SSF spatial scaling factor, AUC area under the curve, CI confidence interval, ROC receiver operating characteristics

\*Numbers in parentheses were used to calculate the percentage

\*\*Largest AUC value in diagnosing specific hepatic fibrosis groups

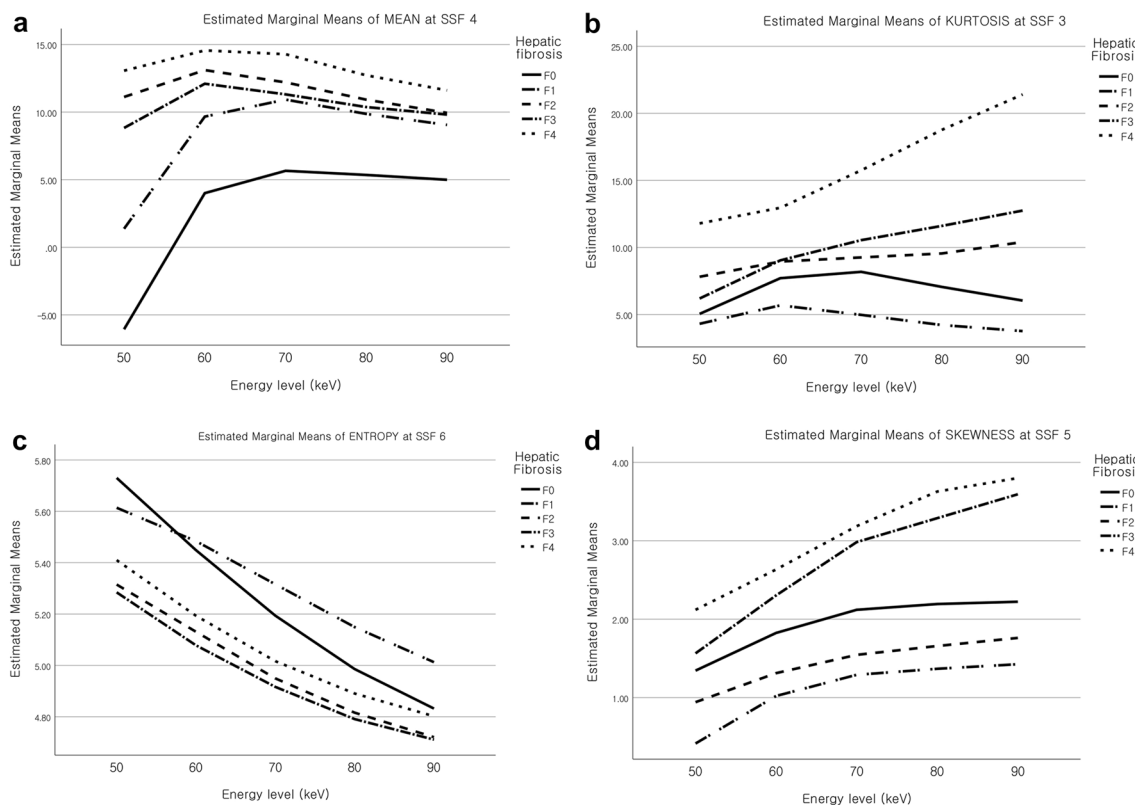


**Fig. 5** Relationships of computed tomography texture analysis (CTTA) parameters with energy level. Estimated marginal means (EMMs) of four parameters [mean gray-level intensity (a), entropy

skewness at medium feature size showed a trend of proportional increase as energy level increased, and advanced fibrosis (F3–F4) was relatively easily distinguished as energy level increased.

### Differences of CTTA parameters between HBV- and HCV-induced hepatic fibrosis

There was no significant difference of CTTA parameters (mean gray-level intensity, skewness, kurtosis, entropy) between HBV-induced hepatic fibrosis and HCV-induced hepatic fibrosis, in all 25 combinations of energy level (50 keV, 60 keV, 70 keV, 80 keV, 90 keV) and SSF [2–6] ( $P > 0.05$ ).

## Discussion

This study demonstrated that CTTA parameters could be feasible and useful imaging biomarkers for evaluation of hepatic fibrosis, and larger differences were obtained when the keV level of VMIs was changed. Clinically significant hepatic fibrosis was significantly characterized by higher mean gray-level intensity, higher kurtosis, and lower entropy.

(b), kurtosis (c), and skewness (d)] tended to show changes as shown in the graphs. In particular, difference in mean gray-level intensity at the 50 keV level was significant

Mean gray-level intensity at the low energy level showed the highest diagnostic performance for diagnosis of fibrosis or clinically significant hepatic fibrosis. These changes in mean gray-level intensity may occur as the homogenous normal background liver develops areas of higher-attenuation fibrosis, collagen, and increased extracellular space [15, 25]. Lubner et al. showed that mean gray-level intensity increased with fibrosis stage, and kurtosis and skewness showed good diagnostic performance for diagnosis of advanced fibrosis [15]. The present study showed similar results that mean gray-level intensity and entropy were meaningful for diagnosis of fibrosis or clinically significant hepatic fibrosis and skewness and kurtosis for advanced fibrosis.

VMIs are generated by application of a monoenergetic beam at a single keV level with attenuation values equivalent to conventional images but with lower artifacts and noise [30]. Depending on the DECT system, VMIs can be generated in either the projection domain (e.g., rapid-kVp-switching DECT) or the image domain (e.g., dual source DECT). Attenuation of iodine is higher at lower energies due to the increased photoelectric attenuation at energies approaching the K-edge of iodine (33.2 keV), and reduction in beam-hardening artifacts is achieved for VMIs at higher keV values [30]. To date, differences in CTTA parameters based on



keV level on DECT have not been reported. In the present study, CTTA parameters showed different values based on keV level. Rassouli et al. reported that CT attenuation of the liver, and spleen was comparable between 70-keV virtual monoenergetic images and conventional 120-kVp images [31]. Mean gray-level intensity showed the most prominent differences among hepatic fibrosis scores at the low energy level, and those at low keV level showed the highest diagnostic performance for diagnosis of clinically significant hepatic fibrosis. These findings are apparently due to an increased iodine attenuation effect at low-keV imaging [30]. However, the estimated marginal means of MEAN dose not proportionally increase. Increasing noise at lower keV VMI and SSF level could be the reason of showing those results. Entropy reflects irregularity and was decreased in reverse proportion to energy level among hepatic fibrosis. As entropy is first-order CTTA parameter which does not consider spatial location or relationship of pixels in ROI, high attenuation change due to fibrosis makes regularity of pixel attenuation [10, 15]. This finding may be due to decreased artifacts at higher keV levels. Kurtosis increases as the variability or heterogeneity of highlighted objects increase, possibly due to fibrosis [29]. Skewness reflects asymmetry of the results [10] and increases proportional to energy level. These differences of CTTA parameters based on keV level could be applicable for CT imaging at low kVp with single-energy CT and for other focal or diffuse liver diseases. Further studies are needed regarding this issue.

Although HBV-induced hepatic fibrosis represent as macronodular type and HCV-induced hepatic fibrosis as micronodular type, all parameters do not show significant difference between them [32–34]. The fact that HBV and HCV share the same histopathologic pattern, or bridging type, of fibrosis progression, might have influence on the similarity of CTTA parameters [35].

Filtration efficaciously smoothens the image, remove all structures at scales smaller than the feature size. By selectively extracting and enhancing features of the image, it could highlight the hepatic textural feature. As the CTTA parameters alter, respectively, according to change of SSF, the results of the analysis on hepatic fibrosis might be affected [23, 29]. In this study, the various significant combinations of parameters and SSF to diagnose clinically significant hepatic fibrosis were obtained and differ according to the parameters. The mean gray-level intensity could be paired with all SSF. On the other hands, kurtosis usually with fine feature size, skewness usually with medium feature size, and entropy is exclusively paired with coarse feature size. Although there is no study dealing with the relationship between SSF and hepatic fibrosis, the optimal SSF might be exist paired with specific CTTA parameter to diagnose hepatic fibrosis and further studies are needed.

The diagnostic performance of the present study showed comparable results compared with those of previous studies [15, 25, 36]. However, this study showed useful information that mean gray-level intensity at the low energy level showed the most prominent differences among hepatic fibrosis compared with those at the high energy level. The VMIs can provided a wide range of energy level without any extra image acquisition. CT is the main follow-up imaging tool for chronic liver disease patients, and it could provide clinically additional information about therapeutic interventions [24]. DECT could lower the radiation dose, compared with conventional single-energy CT and highlight hypervascular lesions [37]. DECT could widen the usage of patients with chronic liver disease.

The feasibility of quantitative evaluation of liver CT for staging liver fibrosis has been evaluated in recent studies [15, 22, 24, 38]. The results showed that CTTA of the liver parenchyma may be a useful non-invasive imaging method for staging hepatic fibrosis. CTTA parameters have the advantage of providing objective and quantitative values. Texture analysis using TexRAD software uses LoG band-pass filters of 2-D isotropic measures of the second spatial derivative of an image; this technique makes it possible to overcome the differences in images arising from use of different CT protocols, including slice thickness, tube current, and voltage, and highlight biologic heterogeneity [10, 25, 39]. Therefore, these parameters could be a useful biomarker for serial examination in patients with parenchymal liver disease; further studies are necessary. Choi et al. reported development of a deep learning system for staging liver fibrosis using portal venous phase liver CT images and showed high diagnostic accuracy compared with previous studies [38]. All these methods require external validation and may not yet be available at many sites.

The present study had several limitations. First, this study was retrospective in design, and selection bias may have existed because we included pathologically confirmed patients with hepatic fibrosis. Pathologic fibrosis stage in this study population was unbalanced. Second, texture analysis was performed on only a single slice of the liver. Although use of a single slice is sufficient for extracting features relevant for clinical application in tumor study [40], further studies are needed in regard to hepatic fibrosis. Third, texture analysis tended to show more noise at lower keV images. A filtration step (LoG spatial band-pass filter) for texture analysis and extraction of limited values from 0 to 300 HU were used to decrease these effects. Forth, the degree of intrahepatic vessel enhancement can affect the results. ROI was manually drawn except major vessels and ribs and any pixels were removed corresponding to areas of fat, air, and major vessels with CT number beyond the range of 0–300 HU. This measurement method was used in previous study of CTTA for the evaluation of hepatic

fibrosis [15]. However, to minimize the effect of intrahepatic vessel enhancement, further studies are needed using other software to remove the effect of segmental branches of vessels. Fifth, the texture analysis was performed on portal phase. However, recent studies shows that extracellular volume fraction, obtained from equilibrium phase image when concentration of iodine contrast is nearly the same among intravascular space and extravascular/extracellular space, significant correlation with liver fibrosis grade [36, 41, 42]. As the portal phase is the ubiquitous phase on abdominal CT imaging [15], it has potential to use as a widely applicable imaging biomarker, and it does not require extra radiation dose for another phase acquisition.

In conclusion, CTTA parameters from different keV levels using a spectral detector CT could be feasible for evaluation of hepatic fibrosis. CTTA parameters from different keV levels demonstrated meaningful accuracy for diagnosis of liver fibrosis or clinically significant hepatic fibrosis. CTTA using TexRAD and DECT appears to be a further step for quantitative and objective evaluation of liver fibrosis, and further research is needed for use in serial examinations.

**Acknowledgements** This research was supported by Korea University Ansan Hospital Grant (O1801331).

**Funding** The authors state that this work has not received any funding.

### Compliance with ethical standards

**Conflict of interest** The scientific guarantor of this publication is Hwan Hoon Chung. The authors of this manuscript declare no relationships with any companies, whose products or services may be related to the subject matter of the article.

### References

1. Heidebaugh JJ, Bruderly M. Cirrhosis and chronic liver failure: part I. Diagnosis and evaluation. *Am Fam Physician*. 2006;74:756–62.
2. Lee SS, Byoun YS, Jeong SH, Kim YM, Gil H, Min BY, et al. Type and cause of liver disease in Korea: single-center experience, 2005–2010. *Clin Mol Hepatol*. 2012;18:309–15.
3. World Health Organization. Global hepatitis report 2017. Washington: World Health Organization; 2017.
4. Friedman SL. Liver fibrosis—from bench to bedside. *J Hepatol*. 2003;38:38–53.
5. Horowitz JM, Venkatesh SK, Ehman RL, Jhaveri K, Kamath P, Ohliger MA, et al. Evaluation of hepatic fibrosis: a review from the society of abdominal radiology disease focus panel. *Abdom Radiol (New York)*. 2017;42:2037–53.
6. Akkaya HE, Erden A, Kuru Oz D, Unal S, Erden I. Magnetic resonance elastography: basic principles, technique, and clinical applications in the liver. *Diagn Interv Radiol*. 2018;24:328–35.
7. Bravo AA, Sheth SG, Chopra S. Liver biopsy. *N Engl J Med*. 2001;344:495–500.
8. Park HJ, Lee SS, Park B, Yun J, Sung YS, Shim WH, et al. Radiomics analysis of gadoxetic acid-enhanced MRI for staging liver fibrosis. *Radiology*. 2019;290:380–7.
9. Low G, Kruse SA, Lomas DJ. General review of magnetic resonance elastography. *World J Radiol*. 2016;8:59–72.
10. Lubner MG, Smith AD, Sandrasegaran K, Sahani DV, Pickhardt PJ. Ct texture analysis: definitions, applications, biologic correlates, and challenges. *Radiographics*. 2017;37:1483–503.
11. Hanania AN, Bantis LE, Feng Z, Wang H, Tamm EP, Katz MH, et al. Quantitative imaging to evaluate malignant potential of ipmns. *Oncotarget*. 2016;7:85776–84.
12. Hu Y, Liang Z, Song B, Han H, Pickhardt PJ, Zhu W, et al. Texture feature extraction and analysis for polyp differentiation via computed tomography colonography. *IEEE Trans Med Imaging*. 2016;35:1522–31.
13. Raman SP, Chen Y, Schroeder JL, Huang P, Fishman EK. Ct texture analysis of renal masses: pilot study using random forest classification for prediction of pathology. *Acad Radiol*. 2014;21:1587–96.
14. Raman SP, Schroeder JL, Huang P, Chen Y, Coquia SF, Kawamoto S, et al. Preliminary data using computed tomography texture analysis for the classification of hypervascular liver lesions: generation of a predictive model on the basis of quantitative spatial frequency measurements—a work in progress. *J Comput Assist Tomogr*. 2015;39:383–95.
15. Lubner MG, Malecki K, Kloke J, Ganeshan B, Pickhardt PJ. Texture analysis of the liver at mdct for assessing hepatic fibrosis. *Abdom Radiol (New York)*. 2017;42:2069–78.
16. Baliyan V, Kordbacheh H, Parameswaran B, Ganeshan B, Sahani D, Kambadakone A. Virtual monoenergetic imaging in rapid kvp-switching dual-energy ct (dect) of the abdomen: impact on ct texture analysis. *Abdom Radiol (New York)*. 2018;43:2693–701.
17. Coursey CA, Nelson RC, Boll DT, Paulson EK, Ho LM, Neville AM, et al. Dual-energy multidetector ct: how does it work, what can it tell us, and when can we use it in abdominopelvic imaging? *Radiographics*. 2010;30:1037–55.
18. Goodman ZD. Grading and staging systems for inflammation and fibrosis in chronic liver diseases. *J Hepatol*. 2007;47:598–607.
19. Chung SR, Lee SS, Kim N, Yu ES, Kim E, Kuhn B, et al. Intra-voxel incoherent motion MRI for liver fibrosis assessment: a pilot study. *Acta Radiol*. 2015;56:1428–36.
20. Ganeshan B, Miles KA, Young RC, Chatwin CR. Hepatic enhancement in colorectal cancer: texture analysis correlates with hepatic hemodynamics and patient survival. *Acad Radiol*. 2007;14:1520–30.
21. Ganeshan B, Miles KA, Young RC, Chatwin CR. In search of biologic correlates for liver texture on portal-phase ct. *Acad Radiol*. 2007;14:1058–68.
22. Bandula S, Punwani S, Rosenberg WM, Jalan R, Hall AR, Dhillon A, et al. Equilibrium contrast-enhanced ct imaging to evaluate hepatic fibrosis: Initial validation by comparison with histopathologic sampling. *Radiology*. 2015;275:136–43.
23. Ganeshan B, Miles KA, Young RC, Chatwin CR. Texture analysis in non-contrast enhanced ct: impact of malignancy on texture in apparently disease-free areas of the liver. *Eur J Radiol*. 2009;70:101–10.
24. Daginawala N, Li B, Buch K, Yu H, Tischler B, Qureshi MM, et al. Using texture analyses of contrast enhanced ct to assess hepatic fibrosis. *Eur J Radiol*. 2016;85:511–7.
25. Lubner MG, Jones D, Kloke J, Said A, Pickhardt PJ. Ct texture analysis of the liver for assessing hepatic fibrosis in patients with hepatitis c virus. *Br J Radiol*. 2019;92:20180153.
26. Varghese BA, Cen SY, Hwang DH, Duddalwar VA. Texture analysis of imaging: what radiologists need to know. *Am J Roentgenol*. 2019;212:520–8.

27. Ganeshan B, Abaleke S, Young RC, Chatwin CR, Miles KA. Texture analysis of non-small cell lung cancer on unenhanced computed tomography: Initial evidence for a relationship with tumour glucose metabolism and stage. *Cancer Imaging*. 2010;10:137–43.
28. Goh V, Ganeshan B, Nathan P, Juttla JK, Vinayan A, Miles KA. Assessment of response to tyrosine kinase inhibitors in metastatic renal cell cancer: Ct texture as a predictive biomarker. *Radiology*. 2011;261:165–71.
29. Miles KA, Ganeshan B, Hayball MP. Ct texture analysis using the filtration-histogram method: what do the measurements mean? *Cancer Imaging*. 2013;13:400–6.
30. Rassouli N, Etesami M, Dhanantwari A, Rajiah P. Detector-based spectral ct with a novel dual-layer technology: principles and applications. *Insights Imaging*. 2017;8:589–98.
31. Rassouli N, Chalian H, Rajiah P, Dhanantwari A, Landaras L. Assessment of 70-kev virtual monoenergetic spectral images in abdominal ct imaging: a comparison study to conventional polychromatic 120-kvp images. *Abdom Radiol (New York)*. 2017;42:2579–86.
32. Baron RL, Gore R. Diffuse liver disease. *Textbook of gastrointestinal radiology*. 2nd ed. Philadelphia: Saunders; 2000. p. 1590–1638.
33. Ohkoshi S, Hirono H, Watanabe K, Hasegawa K, Kamimura K, Yano M. Natural regression of fibrosis in chronic hepatitis b. *World J Gastroenterol*. 2016;22:5459–66.
34. Ros PR, Morteale KJ. Diffuse liver disease. *Clin Liver Dis*. 2002;6:181–201.
35. Hernandez-Gea V, Friedman SL. Pathogenesis of liver fibrosis. *Annu Rev Pathol*. 2011;6:425–56.
36. Sofue K, Tsurusaki M, Mileto A, Hyodo T, Sasaki K, Nishii T, et al. Dual-energy computed tomography for non-invasive staging of liver fibrosis: accuracy of iodine density measurements from contrast-enhanced data. *Hepatol Res*. 2018;48:1008–199.
37. Murray N, Darras KE, Walstra FE, Mohammed MF. Dual-energy ct in evaluation of the acute abdomen. *Radiographics*. 2019;39:264–86.
38. Choi KJ, Jang JK, Lee SS, Sung YS, Shim WH, Kim HS. Development and validation of a deep learning system for staging liver fibrosis by using contrast agent-enhanced ct images in the liver. *Radiology*. 2018;289:688–97.
39. Choi IY, Yeom SK. Feasibility of using computed tomography texture analysis parameters as imaging biomarkers for predicting risk grade of gastrointestinal stromal tumors: comparison with visual inspection. *Abdom Radiol (NY)*. 2019;44:2346–56.
40. Ng F, Kozarski R, Ganeshan B, Goh V. Assessment of tumor heterogeneity by ct texture analysis: can the largest cross-sectional area be used as an alternative to whole tumor analysis? *Eur J Radiol*. 2013;82:342–8.
41. Ito E, Sato K, Yamamoto R, Sakamoto K, Urakawa H, Yoshimitsu K. Usefulness of iodine-blood material density images in estimating degree of liver fibrosis by calculating extracellular volume fraction obtained from routine dual-energy liver ct protocol equilibrium phase data: preliminary experience. *Jpn J Radiol*. 2020;38:365–73.
42. Shinagawa Y, Sakamoto K, Sato K, Ito E, Urakawa H, Yoshimitsu K. Usefulness of new subtraction algorithm in estimating degree of liver fibrosis by calculating extracellular volume fraction obtained from routine liver ct protocol equilibrium phase data: preliminary experience. *Eur J Radiol*. 2018;103:99–104.

**Publisher's Note** Springer Nature remains neutral with regard to jurisdictional claims in published maps and institutional affiliations.